FINAL REPORT

Project Title: **Microstructure and Mechanics of Superconductor Epitaxy via the Chemical Solution Deposition Method**

Covering Period: September 1, 2003 to December 31st 2006

Date of Report: November 2006

Recipient: Materials Department
University of California
Santa Barbara, CA, 93106-5050

Award Number: DE-FC07-03ID14511

Subcontractors: NA

Other Partners: Amit Goyal, goyala@ornl.gov
Paul G. Clem, pgclem@sandia.gov
Quanxi Jia <qxjia@lanl.gov>

Contact(s): Professor Frederick F. Lange
Materials Department
University of California
Santa Barbara, CA, 93106-5050
Telephone (805) 893 8248
Email flange@engineering.ucsb.edu

Project Team: Program Manager John Yankeelov. yankeeja@id.doe.gov
HQ Program Manager Dr. Marshall J. Reed, Marshall.Reed@hq.doe.gov

Project Objective: Research concerns the study of producing thicker epitaxial barrier layers on NiW substrates supplied by ORNL and, latter in the program, IBAD/MgO substrates supplied LANL

Executive Summary: Initially the funds were sufficient funds were awarded to support one graduate student and one post-doc. Lange, though other funds, also supported a graduate intern from ETH Zurich, Switzerland for a period of 6 months. The initial direction was to study the chemical solution deposition method to understand the microstructural and mechanical phenomena that currently limit the production of thick film, reliable superconductor wires. The study was focused on producing thicker buffer layer(s) on Ni-alloy substrates produced by the RABiTS method. It focused on the development of the microstructure during epitaxy, and the mechanical phenomena that produce cracks during dip-coating, pyrolysis (decomposition of precursors during heating), crystallization and epitaxy. The initial direction of producing thicker layers of a know buffer layer material was redirected by co-workers at ORNL, in an attempt to epitaxially synthesize a potential buffer layer material, $LaMnO_3$, via the solution route. After a more than a period of 6 months that showed that the $LaMnO_3$ reacted with the Ni-W substrate at temperatures that could produce epitaxy, reviewers at the annual program review strongly recommended that the research was not yielding positive results. The only positive result presented at the meeting was that much thicker films could be produce by incorporating a polymer into the precursor that appeared to

increase the precursor's resistance to crack growth. Thus, to continue the program, the objectives were changed to find compositions with the perovskite structure that would be a) chemically compatible with either the Ni-W RABiTS or the MgO IBAD Ni-alloy substrates, and produce a better lattice parameter fit between either of the two substrates. The materials examined are show in the following table.

Material	**Lattice* parameter**	**Mismatch with MgO**	**Mismatch with Ni** [c(2x2) sulfur]	**Mismatch with YBCO**
MgO (IBAD Substrate)	**4.210**	0		**9.35%**
$BaZrO_3$	4.193	0.4%		8.8
$SrZrO_3$	**4.101**	**2.6**		**6.5**
$LaMnO_3**$	**3.930**	**6.7**		**2.0**
$SrTiO_3$	3.905	7.2		1.4
$LaGaO_3$	3.874	8.0		0.6
YBCO $**$	**3.850**	**8.6**	**9.4%**	**0**
$LaAlO_3$ $***$	**3.778**		**7.3**	**1.9**
$GdAlO_3$	3.71		5.4	3.6
$YAlO_3$	**3.68**		**4.5**	**4.4**
NiWc(2x2)S (RABiTS Substrate)	**3.520**		0	**8.6%**

At the start of the second year, the funding was reduced to 2/3's of the first year level, which required the termination of the post-doc after approximately 5 months into the second year. From then on, further funding was intermittent to say the least, and funding to support the student and the research expenses has to be supplemented by Lange's gift funds.

During the first part of the second year, strontium zirconate was identified as an alternative to lanthanum manganite as a buffer layer for use on the IBAD MgO superconducting wire. A lattice parameter of 4.101 Angstroms offers a reduced lattice mismatch between the MgO and $SrZrO_3$. Studies were focused on investigating hybrid precursor routes, combining Sr acetate with a number of different Zr alkoxides. Initial results from heat treating precursors to form powders are positive with the formation of orthorhombic $SrZrO_3$ at temperatures between 800°C and 1100°C under a reducing atmosphere of Ar – 5% H_2. Buffer layer research on RABiTS substrates were centered on $GdAlO_3$ (3.71 Å) and $YAlO_3$ (3.68 Å) buffer layer materials. Powder experiments in $YAlO_3$ have shown the perovskite phase to be metastable at processing temperatures below 1500 °C. Experiments involving spin coating of $YAlO_3$ precursors have found significant problems involved with wettability of the $YAlO_3$ precursor (Yttrium acetate, Aluminum tri-sec butoxide, DI water and Formic Acid) on RABiTS substrates; this, and the demise of the funds precluded further research using $YAlO_3$.

The diminished funds for the second year, and the small, tricked funds during the third year lead to a redirection of the student to another research area., and a stop to any experimental achievements that were much too ambition relative to the available funds.

The only positive results obtained during this latter period was the understanding why two dissimilar structures could result in an epitaxial relation. It was shown that two rules of crystal chemistry, cation/anion coordination and charge balance, could be applied to understand the epitaxy of $SrTiO_3$ on Ni *c*(2 X 2)S, TiO_2 (anatase) on $LaAlO_3$, TiO_2 (rutile) on *r*-plane Al_2O_3, and $Zr_{1-x}(Y_x)O_2$ on (0001) Al_2O_3. This new understanding of the interface between two dissimilar structures has important implications that include the buffer layers used for the superconductor program, namely, the epitaxy of perovskites such as the epitaxy of $SrTiO_3$ on the Ni *c*(2 X 2)S wire. This discovery is the major part of the finial report that follows.

Crystal Chemistry of Interfaces Formed Between Two Dissimilar Structures

David Andeen and F. F. Lange
Materials Department
University of California at Santa Barbara

Abstract

Epitaxial relations are often described by the mismatch of lattice parameters between the two materials. When the structures forming the epitaxial interface are dissimilar, the lattice mismatch is often less meaningful because of the different geometrical arrangement of atoms in the two structures. In a previous paper, [1] it was shown that two rules of crystal chemistry, cation/anion coordination and charge balance, could be applied to understand the epitaxy of (0001) ZnO (wurtzite) on (111) $MgAl_2O_4$ (spinel) substrates. More recently, it was shown that the same rules could be applied to predict and confirm the epitaxy of (101) SiO_2 (cristobalite) on (0001) Al_2O_3 (sapphire). [2] Here, the same rules are applied to understand the epitaxy of four other dissimilar structures that have been previously published by others, including $SrTiO_3$ on Ni *c*(2 X 2)S, [3, 4] TiO_2 (anatase) on $LaAlO_3$, [5] TiO_2 (rutile) on *r*-plane Al_2O_3, [5] and $Zr_{1-x}(Y_x)O_2$ on (0001) Al_2O_3. [6]

1.0 Introduction

Without a doubt, when one crystalline material is allowed to nucleate and grow on another, special crystallographic relations are discovered that would not be predicted with any current theory. There are many examples; some are used in industrial processes. One of the more interesting examples occurs when a small amount of P_2O_5 is added to a silicate melt that will form a lithium-silicate glass. The P_2O_5 is known to 'seed' the homogeneous nucleation of three phases, lithium metasilicate (Li_2SiO_3), lithium disilicate ($Li_2Si_2O_5$), and cristobalite (SiO_2), to produce a useful glass ceramic (a material first formed as a glass and then converted into a polycrystalline ceramic via a heat treatment). Seminal transmission electron microscopy (TEM) studies of T. J. Headley and R. E. Loehman [7] showed that lithium orthophosphate (Li_3PO_4) homogeneously nucleates during cooling. When the glass is held at a 'nucleating temperature,' they showed that three different crystalline phases nucleate on the surface of the Li_3PO_4 crystallites, each with a different preferred orientational relation. In other words, each Li_3PO_4 crystallite acts as a 'seed' for the epitaxial growth of all three silicates, each with a different crystal structure, all of which differ from that of the Li_3PO_4. Like all other discoveries of 'special' epitaxial relations between dissimilar (and similar) crystalline structures, Headley and Loehman explain their discovery by showing that, in the interface between the two structures, the spacing between lattice sites in one structure is similar to the spacing between lattice sites in the adjoining structure. The differential lattice spacing divided by the lattice spacing of one of the two structures is generally called the lattice misfit strain. In general, although the lattice misfit strain can be as large as 16% [the case of GaN on basal plane (0001) sapphire], most lattice misfit strains are less than 10%; those reported by Headley and Loehman were ≤ 5%.

For identical structures with different lattice spacings, the misfit strain can be conceptually related to the excess energy associated with the interface, due to the predictable dislocation density at the interface. This conceptual relation is not apparent for different structures, [1] and thus differential strain cannot be the only tool used to explain special crystallographic relations.

The coincident site lattice (CSL) model has often been used to understand the frequent occurrence of interfaces between two lattices.[8] It was first used to understand the interfaces that join together two identical crystals, namely grain boundaries. The CSL model was of limited success in predicting the formation of special grain boundaries in metals, in which two identical crystals form an interface. With this limited success, it has been assumed that the plane with the largest number of coincident sites might have the lowest free energy. Later, the CSL model has been used to explain the special interfaces observed between two crystals with dissimilar structures.[9,10] When applied to dissimilar structures, the requirement for exact coincidence of lattice sites is usually relaxed, such that when lattice vectors in the two structures are compared, some misfit is allowed, giving rise to the term near coincident site lattice (NCSL) model.

Determining a CSL (or NCSL) starts by rotating the two lattices about an invariant direction (normal to the interface) to seek a plane(s), via a computer search, with the greatest density of coincident lattice sites, i.e., sites in one lattice that overlay sites in the second lattice. To this end, in the near coincidence site lattice (NCSL) principle, translation vectors in both lattices need not perfectly match one another. It was anticipated that planes with the largest density of coincident sites (or near coincident sites) would have a low interfacial energy. Although CSL (or NCSL) representations can be formed with known epitaxial relations between dissimilar structures, other possible, however, not observed, NCSL relations can be formed with the same invariant rotational axis that produces identical coincident site densities with similar misfit allowances.[6] Thus, the NCSL model cannot necessarily predict an epitaxial relation even when the invariant rotation axis is known.

Recently, the current authors discovered that the two simple rules of crystal chemistry can be used to understand epitaxial orientation relations between dissimilar structures. The first rule pertains to the fact that the cations are coordinated by a specific number of anions, referred to as the coordination number, which depends on the size ratio of the cations to anions. The current authors hypothesized that this first, and most important, rule must be obeyed across an interface. The second rule states that the charge associated with the cations and anions within a space that describes the structure (usually known as the unit cell), should balance. These two rules are commonly used to select a stable of different cations and anions that substitute for one another to form specific structures.

Two aforementioned interfaces, ZnO on $MgAl_2O_4$ [1] and cristobalite (SiO_2) on Al_2O_3,[2] demonstrate how the two rules of crystal chemistry are applied. In the case of (0001) ZnO epitaxy on (111) spinel ($MgAl_2O_4$), zinc atoms, at the interface, sit in sites normally occupied by magnesium and aluminum. These sites, with three oxygen atoms from the spinel and one from the ensuing ZnO oxygen layer above, provide the necessary 4-fold coordination of oxygen atoms, which is most commonly observed for zinc. It was hypothesized that the charge balance can be achieved with the presence of protons, readily available from the aqueous growth solution, that coordinate two opposing oxygen atoms across the interface. In the case of cristobalite on (0001) sapphire (Al_2O_3), silicon atoms occupy sites normally occupied by aluminum atoms. The sites provide three in-plane oxygen atoms, which ultimately form tetrahedral coordination when capped with the ensuing layer of oxygen atoms. Charge balance is achieved because three silicon atoms substitute in place of four aluminum atoms, thereby accumulating the same charge per unit area of interface.

The objective here is to show how these two crystal chemistry rules can be used to explain four different epitaxial relations previously reported by others. The relations include $SrTiO_3$ (perovskite) on Nickel *c*(2 X 2)S,[3, 4] TiO_2 (anatase) on $LaAlO_3$ (perovskite),[5] TiO_2 (rutile) on *r*-plane sapphire,[5] and $Zr_{1-x}(Y_x)O_2$ (fluorite) on *c*-plane sapphire.[6] The application of the two rules of crystal chemistry serves to demonstrate a different characteristic of epitaxy in each case and lend insight into the epitaxial interfaces that are formed.

2.0 Strontium Titanate on Nickel *c*(2 X 2)

It was discovered that rolling-assisted biaxially textured substrates [RABiTS] of {100}< 100> Ni thin foil could be used to produce a 'near' single crystal substrate for the epitaxy of different oxide buffer layers followed by an epitaxial layer of the $YBa_2Cu_3O_{7+d}$ superconductor.[11] Cantoni et al [3, 4] recognized that to achieve consistent processing of epitaxial buffer layers of either $Zr_{1-x}(Y_x)O_2$, CeO_2, or $SrTiO_3$, on the Ni, required a heat treatment to allow the formation of a *c*(2 X 2), two-dimensional superstructure of sulfur [12] formed by the surface segregation of the sulfur contained within the Ni foil. Cantoni *et al* [4] proposed "…that the role played by the S superstructure can be partially explained on the basis of structural and chemical considerations. The S layer behaves like a template that matches and mimics the arrangement of the oxygen atoms in particular (001) sub-lattice planes considered in this study [Y_2O_3-stabilized ZrO_2 (YSZ), CeO_2, and $SrTiO_3$]. Sulfur belongs to the VI group and is chemically very similar to oxygen, often exhibiting the same electronic valence." Therefore, it is plausible that during the seed layer deposition the cations easily bond to the S atoms already present on the substrate surface, giving rise to the (001) epitaxial growth of the film, which otherwise would not take place.

Here, for the specific case of epitaxial $SrTiO_3$, we add to this explanation to show that the sulfur is positioned on the (100) Ni surface to allow the smaller cation, Ti, to fill a 6 fold coordinated site with its surrounding cations, namely, 5 oxygen atoms and one sulfur. Although not detailed here, S plays the same role for the other epitaxial films. As shown in Fig. 1, the two-dimensional superstructure of sulfur is similar to that of the titanium layer in the deposited $SrTiO_3$. The sulfur atoms then coordinate the bases of the titanium-centered octahedra in the $SrTiO_3$, as shown in Fig. 2, which is scaled, for the sake of clarity, so that the separation between the oxygens in the $SrTiO_3$ structure and the sulfur in the *c*(2 X 2) layer is zero.

The system cannot be charge balanced from a purely ionic standpoint because nickel is a metal. The bonding in the sulfur *c*(2 X 2) layer, however, slightly resembles that in the hexagonal NiS structure. Within NiS, both nickel and sulfur are octahedrally coordinated by each other. Therefore, in the ionic limit, they would transfer 1/6 of their charge, or ±1/3, to each nearest neighbor. If the bonding is similar in the sulfur *c*(2 X 2) layer on the nickel, each sulfur atom, with its four nickel nearest neighbors, would transfer –1/3 to each, for a total of –4/3. The remaining –2/3 of charge would then be transferred to the titanium in the epitaxial $SrTiO_3$ layer above, which has a +4 valence and requires –2/3 from each nearest neighbor when octahedrally coordinated, in the ionic limit. Hence, both crystal chemistry rules, namely cation coordination and charge balance, are observed at the interface.

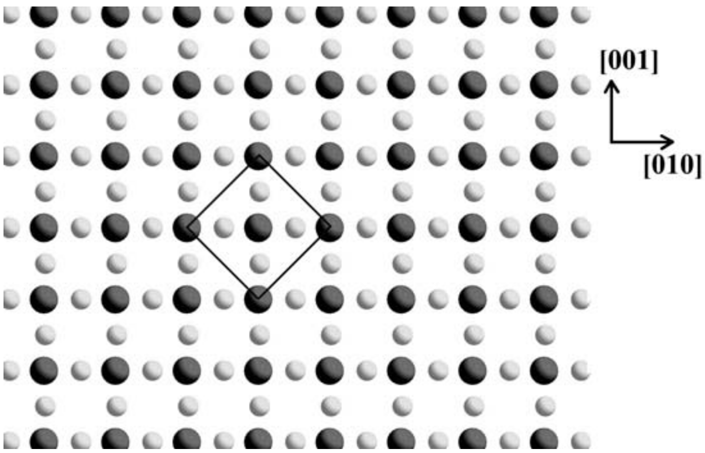

Fig. 1. (100) Nickel *c*(2 X 2)S, represented by the small, light balls. Large, dark balls represent the *c*(2 X 2) sulfur layer, whose unit cell is marked with black lines.

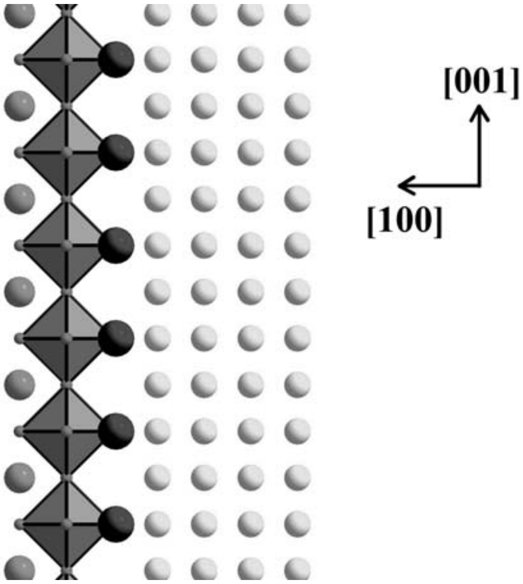

Fig. 2. Epitaxial $SrTiO_3$ on (100) Ni *c*(2 X 2)S, the octahedrons are titanium-centered and bonded to oxygen atoms on all sides except for the interface side, which is bonded to sulfur, as represented by the large, dark balls between the titanium octahedrons and the bulk nickel, represented by the small, light balls on the right. Strontium atoms terminate the $SrTiO_3$ layer. The model is scaled such that the distances between the oxygen atoms that terminate the octahedra in SrTiO3 and the distance between the S atoms in the superstructure are identical. In reality, the mismatch between these is approximately 10%. Crystallographic directions refer to both structures.

3.0 Anatase on $LaAlO_3$

The work of Huang *et al.* [5] resulted in the stable deposition, by pulsed laser deposition, of anatase (TiO_2) on (001) $LaAlO_3$ at 800ºC. Although anatase is the low temperature polymorph of TiO_2, Huang *et al.* concluded that "…the similarity of the O groups at the interface planes is believed to be crucial in determining the phase formation and the epitaxial growth of the films." In addition, their clear transmission electron microscopy (TEM) observations, coupled with interface simulations, reveal an interface terminated by the La layer of the $LaAlO_3$, rather than the Al layer in the perovskite.

Here, we will use the rules of crystal chemistry to discuss how the La-terminated layer provides the ideal interface for both the structural match of the epitaxial anatase and the cation coordination of the ensuing titanium octahedra. Further, using the concept of charge balance, we predict that under equilibrium conditions, La vacancies are expected to exist at the interface. As a result, any other interfacial scenarios will be clearly unlikely due to the necessary face and edge sharing of the involved polyhedra and the difficult charge balancing that would ensue.

Before describing the interface, each structure will be presented for clarity. $LaAlO_3$ is a rhombohedral structure that is often represented as a pseudocubic structure. The rhombohedral indexing will be used followed by the cubic indexing in parentheses for completeness. Along the $[1\bar{1}1]$ direction, ([001] in its high temperature cubic polymorph**)**, the structure consists of alternating planes of lanthanum and oxygen, and planes of aluminum and oxygen. The aluminum atoms sit in octahedral sites, while the lanthanum atoms sit in dodecahedral sites, coordinated by 12 nearest neighbor oxygen atoms. The aluminum octahedra share corners in all three directions and create a "chess board" appearance when viewed along the $[1\bar{1}1]$ direction, ([001] in its cubic polymorph), as shown in Fig. 3(a). The side view of the structure along the $[10\bar{1}]$, ([100] in cubic), is pictured in Fig. 3(b), which shows the alternating layers of aluminum-centered octahedra and lanthanum/oxygen layers.

The anatase form of TiO_2 has a tetragonal symmetry. Parallel to the [001] direction, the structure consists of sheets of mixed oxygen and titanium atoms. The oxygen atoms octahedrally coordinate the Ti atoms to form layers of corner sharing octahedra in the (001) plane. When a single layer of octahedrons are viewed along the [001] direction, as in Fig. 4(a), the structure has the "chess board" appearance similar to that of $LaAlO_3$ in the $[1\bar{1}1]$ direction, ([001] in cubic). In addition to sharing corners within the (001), the octahedra share edges with similar layers out of the (001) plane. The respective layers of octahedra are therefore displaced from each other by approximately one-quarter lattice constant in the [001] direction and one-half lattice constant in either the [100] or [010] directions. The result is that every oxygen atom is attached to three octahedra. A side view of the structure along the [100], as shown in Fig. 4(b), reveals that the octahedra are slightly distorted as the oxygen atoms of each layer are slightly offset from each other.

From a crystal chemistry perspective, epitaxy is most likely to occur such that the octahedral layers of both materials share corners. By terminating the $LaAlO_3$ with a layer consisting of lanthanum and oxygen, as shown in Fig. 3(b), the anatase then grows with the two structures sharing the interfacial layer of oxygen atoms. In this case, both titanium and aluminum remain eight-fold coordinated and the octahedra continue to share corners. In addition, the lanthanum atoms continue to be twelve-fold coordinated by the oxygen.

In order to charge balance the interface, two charge balanced unit cells must be placed together to form the epitaxial interface. Any anomalies, such as structural misalignment or half atoms, must be adjusted to balance charge so that the entire unit is neutral. The unit of $LaAlO_3$ is outlined in Fig. 3(a) by black and white lines. It is terminated at the lanthanum-oxygen layer, which is the proposed interface, as shown in Fig. 3(b). The unit consists of two lanthanum atoms (two halves on each of two sides), two aluminum atoms (four quarters from the side edges, and two halves on each long side), and six oxygen atoms (eight corners, eight side edges, four faces, and one complete interior atom). The unit of TiO_2 is outlined in Fig. 4(a), also by black and white lines. It is actually two unit cells of TiO_2, stacked in the [010], offset by –1.97Å in the [001] so that it terminates with four oxygen atoms at the corners of the interface, as does the $LaAlO_3$, in the manner that epitaxy is proposed. The TiO_2 unit consists of eight titanium atoms (four edges, eight faces, and three interior atoms) and sixteen oxygen atoms (eight corners, eight edges, fourteen faces, and six interior atoms). The length of the anatase unit cell in the [001] is necessary because the octahedral layers repeat only every fourth layer.

When the two units are placed together, the oxygen atoms line up almost perfectly which reflects the low in-plane lattice mismatch of 0.21% between the oxygen atoms in the adjacent planes of both structures. At the interface, however, lie two half-lanthanum atoms, which will not exist in a real crystal. Removing both half atoms, and replacing them with a single lanthanum atom plus a vacant lanthanum site produces a charge balance. The new interfacial layer, pictured in Fig. 5, consists of lanthanum atoms at the interface located in one half of their usual sites and the other half vacant sites. A high resolution TEM image along the $LaAlO_3$ [110] might provide experimental confirmation of the proposed interface, however, Huang *et al.* did not report these vacant sites in their TEM imaging work. Lack of experimental evidence of vacancies may be a result of many reasons, including a charged, non-equilibrium interface, as experimentally observed for $LaAlO_3$ on $SrTiO_3$.[13]

The in-plane lattice mismatch of 0.21% makes for a favorable growth relationship. In addition, this epitaxial relationship has favorable out-of-plane mismatches that likely stabilize the anatase and favor its epitaxy. The distance from titanium to nearest aluminum across the interface becomes 3.862Å, a mismatch of only 1.8% compared to the aluminum-to-aluminum distance in $LaAlO_3$. In addition, the titanium to nearest lanthanum distance, again across the interface, becomes 3.325Å, a mismatch of 1.2% compared to the lanthanum-to-aluminum distance in $LaAlO_3$. The distances from lanthanum at the interface to the first oxygen layer of the anatase are 2.451Å and 3.042Å, while the bulk lanthanum-to-oxygen distance is 2.682Å. Despite this variation, the average lanthanum-to-oxygen distance becomes 2.747Å, which results in a mismatch of 2.4% compared to the bulk $LaAlO_3$.

Other epitaxial interfaces are certainly possible in this system from a geometrical standpoint. These other interfaces, however, result in close cation-to-cation distances because of the proximity of Ti atoms in the [001] direction of the anatase, a result of edge sharing octahedra in that direction. This would also result in a scenario requiring complicated edge sharing of the octahedra across the interface.

Although edge sharing occurs in the anatase, it does not in the $LaAlO_3$. Such a result would change the anion coordination of cations. It is contrary to both the first rule of crystal chemistry and to the experimental TEM images of Huang *et al*. as previously discussed.

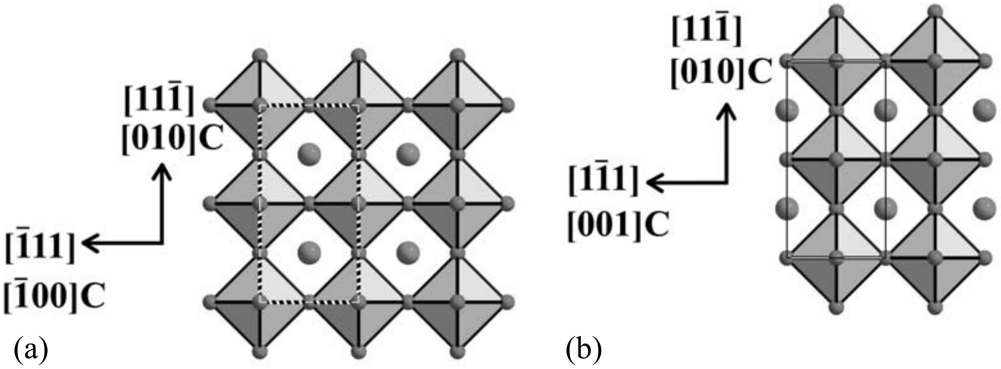

Fig. 3. (a) View of $LaAlO_3$ with the [1$\bar{1}$1] ([0C[illegible] [illegible]bic coordinates, and designated by a 'C') direction coming out of the page. The squares represent aluminum-centered octahedra, while the individual dots are lanthanum atoms. (b) View of the $LaAlO_3$ with the [10$\bar{1}$] ([100] in cubic coordinates) coming out of the page. Two layers of the material are shown, terminating on both sides with a lanthanum and oxygen layer.

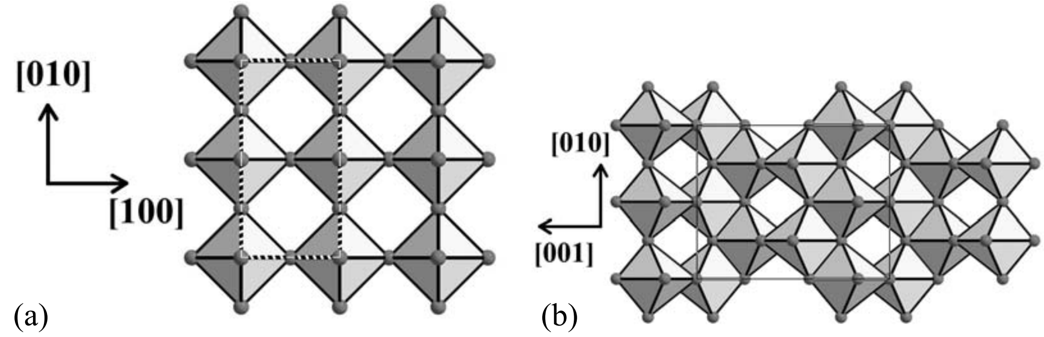

[illegible] a) Representation of anatase TiO_2 as [illegible] centered octahedra, [001] direction is coming out of the page, only a single layer of octahedra are shown. (b) View of anatase with [100] coming out of the page.

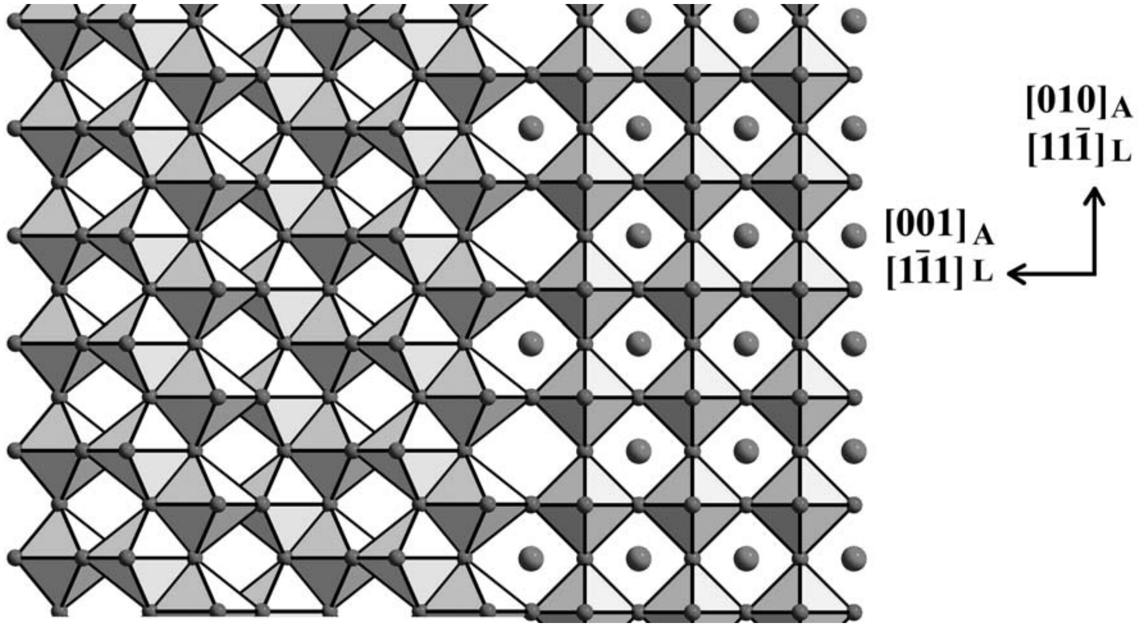

Fig. 5. Side view of the $LaAlO_3$/anatase interface, featuring corner sharing between aluminum and titanium octahedra as well as lanthanum vacancies. Crystallographic directions for anatase and $LaAlO_3$ are indicated by 'A' and 'L' respectively.

4.0 Rutile on *r*-plane Sapphire

The third interface was also grown by Huang *et al.* [5] and consists of TiO_2 (rutile) on *r*-plane Al_2O_3. The TEM images reported by Hung *et al.* show that the cations at the interface are sandwiched between to layers of oxygen atoms, which the author suggest were "…an appropriate atomic pattern…" for the seeding of the rutile phase. As described below, the two sandwiching planes of oxygen atoms mimic layers observed in the two different structures, which allows both corner and edge sharing of the octahedra needed to span the interface. Ultimately, despite a short-range charge imbalance, the similarity of the interface between the two different structures results in charge balance without any atomic rearrangement.

Sapphire is a material used frequently as a substrate for the epitaxial growth of many different materials. The structure is rhombohedral and consists of close packed oxygen planes with aluminum sitting in two thirds of the available octahedral sites. When viewed along the $[11\bar{2}0]$, which shows the cross-section of the R-plane, the structure consists of five layers of atoms that repeat that sequentially repeat to form the structure. The atoms within each of these five layers stack in the following sequence: oxygen, aluminum, oxygen, aluminum, and oxygen, as represented in Fig. 6(a). Because the aluminum ions sit in octahedral sites, the structure is easier to visualize when viewed as two different repeating layers of aluminum centered octahedrons. Each octahedron shares one face and two edges with the layer closest to it, thus forming an aluminum-rich stack in which two layers of aluminum atoms sandwich one layer of oxygen atoms. Each octahedron then shares one edge with the layer on the other side, thus forming an oxygen-rich stack in which two oxygen layers are immediately next to each other. The octahedrons shown in Fig. 6(a) are a pair of layers that are sharing faces and would share edges with layers adjacent to them on either side.

Within each layer of the *r*-plane, the octahedrons share only corners, as shown in Fig. 6(b). In addition, each layer consists of octahedrons pointing in one of two directions. Repetition of those two octahedrons will produce a complete layer. The repetition of these two face-sharing layers of octahedrons forms the structure in the direction perpendicular to the r-plane.

On the other hand, rutile is a tetragonal structure. When viewed along the [100], the structure consists of two layers of oxygen atoms, sandwiching a layer of titanium atoms, as shown in Fig. 7(a). The titanium atoms sit in octahedral sites and the structure consists of layers of octahedrons. Every octahedron shares two edges, one with each layer on either side of it along the [100]. The oxygen along the shared edges of the octahedrons then form the oxygen rich stacks between the layers of titanium atoms. Fig. 7(a) also shows a single layer of titanium octahedrons. Within each layer of octahedrons, all the octahedrons share corners, as shown in Fig. 7(b). The layer also consists of octahedrons pointing in one of two directions, similar to the layers in sapphire.

Epitaxy of rutile on *r*-plane sapphire will occur with a layer of rutile octahedrons growing on a layer of sapphire octahedrons. The interface will be composed of the two oxygen layers, as observed experimentally. [5] These layers comprise the oxygen rich stack that would normally exist in the sapphire structure, as well as in the rutile structure. In both structures, the oxygen-rich stack contains the shared edges of octahedra, one from each side. Other epitaxial orientations would require unfavorable face sharing of rutile octahedra with sapphire octahedra.

The epitaxy is best described by first showing how two edge-sharing octahedral layers in sapphire are oriented, as illustrated on the left side of Fig. 8. Note, again, that each layer of sapphire consists of octahedra with two different orientations, which may be differentiated by observing the direction the axis of the octahedron is pointing. One type of octahedron is labeled ‘A’ and the other is labeled ‘B.’ In the next layer of sapphire, the octahedron labeled ‘a’ will share its bottom edge with the highlighted (by the contrasting black and white line) edge of the octahedron labeled ‘A.’ The same edge sharing will also occur for octahedra labeled ‘B’ and ‘b.’

Epitaxy of rutile on sapphire will occur as illustrated on the right side of Fig. 8. The first rutile octahedron, labeled ‘1,’ will share an edge with the octahedron in the adjacent sapphire structure, labeled ‘A’. This is the same edge that is normally shared by the octahedron labeled ‘a’ in the bulk sapphire. The second rutile octahedron, labeled ‘2’, will also share an edge with the sapphire, labeled ‘B,’ also the same edge that would normally be shared by the octahedron labeled ‘b’ in the sapphire structure. In addition, each octahedron shares an oxygen atom with an adjacent octahedron. Overall, the rutile octahedrons will share the same edges and corners with the sapphire that the subsequent layer of octahedrons in a sapphire structure would share, thus preserving the coordination of cations across the interface, in both structures.

The two structures share a similar shaped repeatable unit, namely, their oxygen octahedrons, with which they share edges at the interface as illustrated in Figs. 6(b) and 7(b). The mismatch for the interatomic distance in which the two types of octahedrons that share edges, the Ti-octahedrons and Al-octahedrons, at the interface is more than likely the best description of the ‘lattice mismatch’. The edge of the Al-octahedron is 2.62Å, while the edge of the Ti-octahedron is 2.54Å, suggesting a mismatch of – 3.1%.

The final step in this crystal chemistry analysis is charge balancing. The polyhedral model of the two materials indicates that each oxygen atom in a sapphire octahedron is shared among four octahedrons. In the case of the rutile, each oxygen atom is shared by three octahedrons. The interface layer then requires certain oxygen atoms to be shared between both aluminum-centered octahedra and titanium-centered octahedra. In the interfacial layer, the oxygen atoms closer to the bulk sapphire will be shared among three aluminum-centered octahedra and one titanium-centered octahedra. This will result in excess positive charge, +1/6 per oxygen atom. On the other hand, the interfacial oxygen atoms closer to the epitaxial rutile will be shared by one aluminum-centered octahedra and two titanium-centered octahedra. This will result in excess negative charge, -1/6 per oxygen atom. Because there are an equal number of oxygen atoms on either side of the interfacial layer, these local charge imbalances will cancel out, resulting in a locally charge balanced interface.

The black and white lines in Figures 6 and 7 outline the unit cells chosen for a bulk charge balance exercise. The sapphire unit cell consists of two five-layer units that make up a repeating layer of material. This unit cell contains 12 oxygen atoms (4 edges, 4 faces, and 9 complete atoms) and 8 aluminum atoms (8 complete atoms) that make up a charge balanced unit cell. The rutile unit cell consists of one three-layer unit that makes up the repeating layer of the material. This unit cell contains 4 oxygen atoms (4 edges, 2 faces, and 2 complete atoms) and 2 titanium atoms (2 complete atoms), which also results in a charge balanced unit. Placing the two units together requires no vacancies or extra atoms. The bulk unit is charge balanced, and only the previously mentioned local charge imbalance exists.

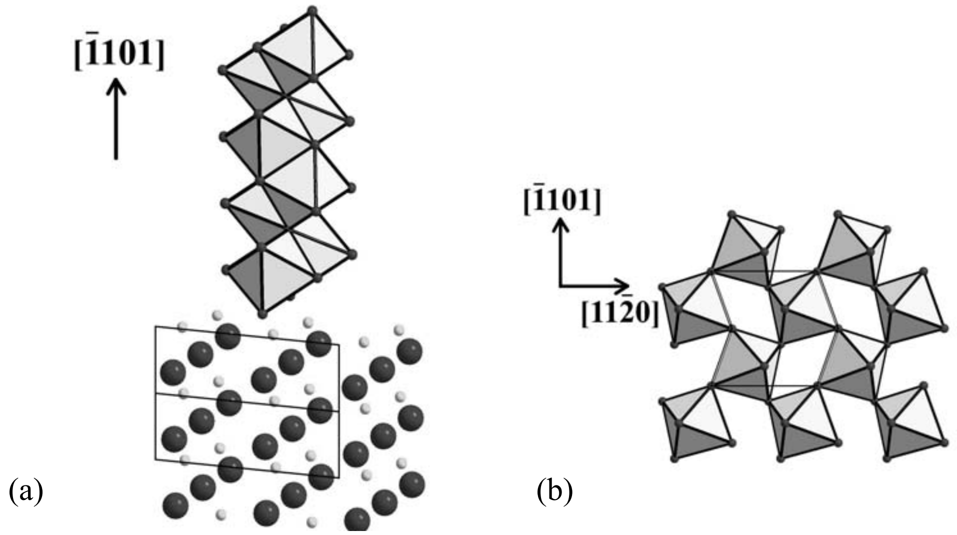

Fig. 6. (a) Cross sectional view of sapphire *r*-plane $(\bar{1}10\bar{2})$ with the $[11\bar{2}0]$ coming out of the page, octahedra are aluminum-centered. Small, light balls represent aluminum, while large, dark balls represent oxygen. (b) View of a single layer of octahedrons of the *r*-plane, black and white lines mark the outline for the unit cell selected for charge balance

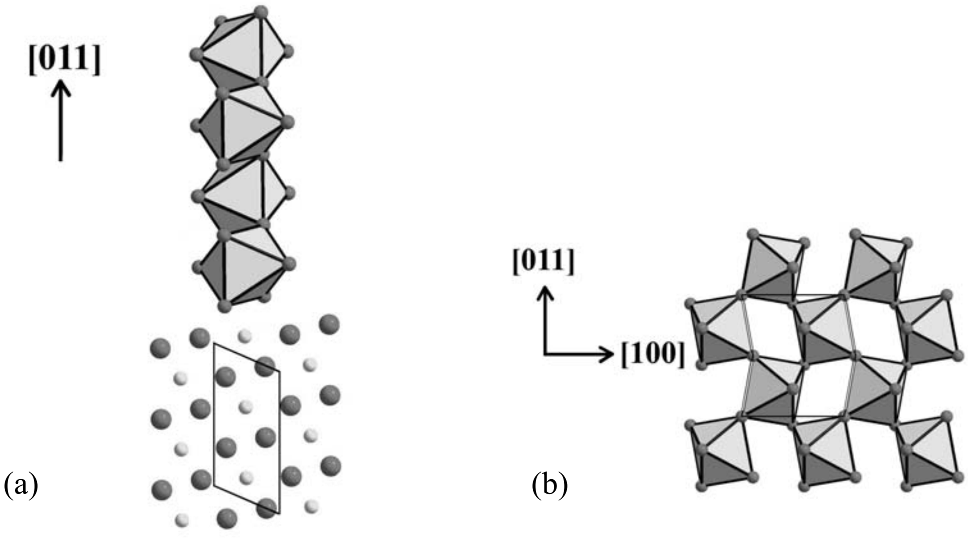

Fig. 7. (a) Cross sectional view of the TiO_2 rutile (011) with the [100] coming out of the page, octahedra are titanium-centered. Small, light balls represent titanium, while large, dark balls represent oxygen. (b) View of the rutile $(0\bar{1}1)$, as in Fig. 3, black and white lines mark the outline for the unit cell selected for charge balance

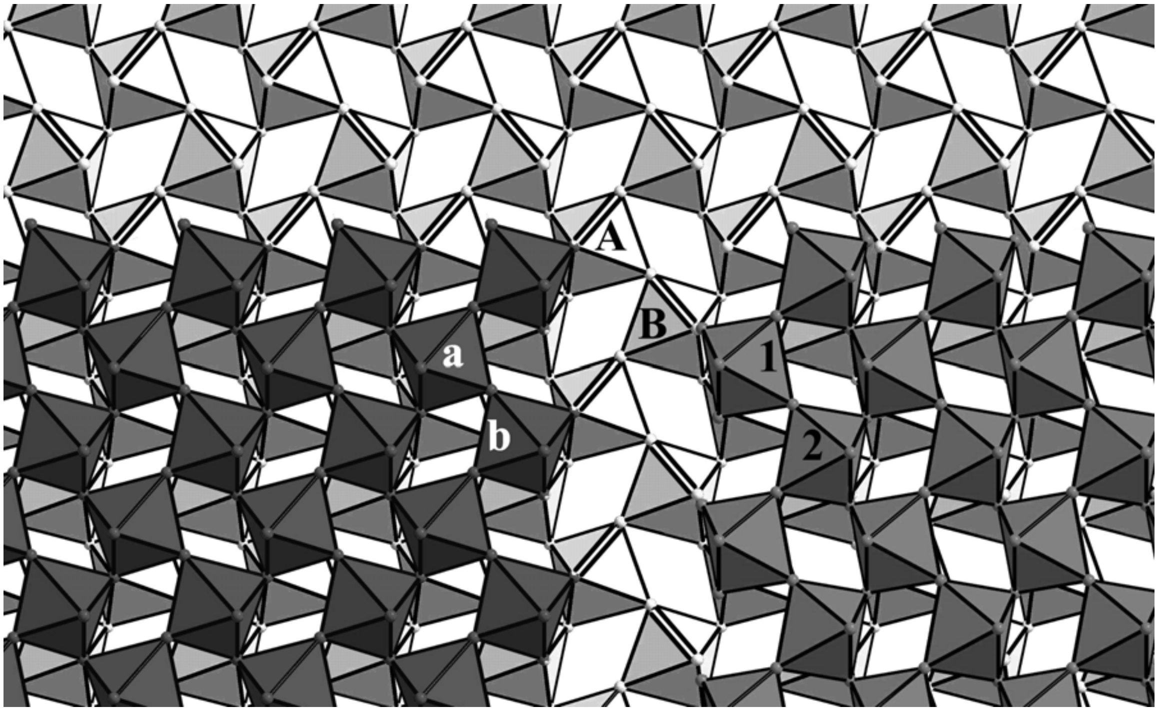

Fig. 8. Octahedral representation of the sapphire *r*-plane (light octahedra), the dark octahedra on the left are bonded to the layer as they would in bulk sapphire, the medium-gray octahedra on the right are the rutile $(0\bar{1}1)$ as they would bond to the sapphire and form an epitaxial layer. Contrasting lines show the edges that are shared between the octahedra in both interfaces.

5.0 Cubic Zirconia on C-plane Sapphire

The work of Cain *et al.* [6] was initiated for the very purpose of understanding the nature of epitaxial relationships, both out-of-plane and in-plane, for $Zr(Y)O_2$ with the cubic, fluorite structure on different sapphire substrates. Experimental and NCSL results for $Zr(Y)O_2$ on both *c*-plane and *a*-plane sapphire defined a number of epitaxial orientations. Here, we will focus on only one, namely the that of $Zr(Y)O_2$ on (0001) sapphire. The NCSL model was employed to elucidate possible in-plane orientations. In addition to confirming the experimentally observed in-plane orientation, the model predicted another orientation, with identical likelihood, that was not observed.

The NCSL model indicates 6 likely epitaxial orientations for cubic ZrO_2 on *c*-plane sapphire. According to NCSL calculations, each orientation has equal values of percentage misfit, δ, and number of unit cells within the larger NCSL cell, σ. Both of these values are calculated to assess the quality of an NCSL match, lower values of each variable are preferable. Each of the six possible NCSL orientations represents one of two in-plane orientations:

$[100]_{ZrO2} \parallel <\bar{1}2\bar{1}0>_{Al2O3}$
or
$[180]_{ZrO2} \parallel <\bar{1}2\bar{1}0>_{Al2O3}$

Namely, the NCSL concept predicts two sets of in-plane orientations, each with three variants due to the 3-fold rotational symmetry about the c axis of sapphire. The first orientation is observed experimentally at three different in-plane angles, while the second orientation is not experimentally observed at all.

Relative to the crystal chemistry approached detailed here, it is interesting to note that zirconia prefers to be coordinated by 7 oxygen ions, but the cubic fluorite structure imposes a coordination of 8 oxygen ions. [14] As detailed below, our proposed interface indicates that zirconium cations at the interface will be coordinated by 7 oxygen atoms. This results in an interface in which all cations are properly coordinated; in addition, the interface is charge balanced.

In this case of epitaxy, the coordination, by anions, of the cations in the two respective structures, sapphire and cubic fluoride zirconia, is completely different. In sapphire, the aluminum atoms are octahedrally coordinated by oxygen. The octahedrons are oriented such that the basal plane of sapphire is terminated as a hexagonal array of oxygen atoms. On the other hand, in its most symmetric form, the fluorite structure is cubic, where the zirconium atoms are coordinated by 8 oxygen atoms, forming a cube to coordinate each zirconium atom centered within the cube. On the (001) surface of the cubic fluoride structure, each cube is terminated as a square. Simply stated and as detailed below, it can be seen that when the zirconium atoms are properly placed between the two planes of oxygen, i.e., one terminated in triangular arrays of oxygen, and one terminated in square arrays of oxygen, the zirconium atoms will be coordinated by 7 oxygen atoms.

Figure 9 shows a single layer of octahedrons that constitute basal plane sapphire. At the interface between the two structures, a layer of zirconium atoms that form the (001) plane of Zr_2O lies above the layer of oxygen atoms. These zirconium atoms are oriented in the $[100]_{ZrO2} \parallel <\bar{1}2\bar{1}0>_{Al2O3}$ epitaxial relationship. Along the $[11\bar{2}0]$ direction the lattice mismatch is 7.4%, relative to the oxygen separation distances within the two structures, while along the $[\bar{1}100]$ direction the mismatch is -6.9%. Despite a clear lattice mismatch, periodic sites appear that could be occupied by zirconium atoms. To improve the visual symmetry, Fig. 10 was constructed by contracting the cubic fluoride structure in the $[100]_{ZrO2}$ direction, and expanding the structure in the $[010]_{ZrO2}$ direction. Triangular sites are clearly visible in Fig. 10, highlighted in translucent, dark gray, with three oxygen atoms from the sapphire coordinating a zirconium atom near the center of each triangle. Since zirconium atoms strongly prefer seven-fold coordination sites, [14] the sites shown in Fig. 10 are ideal for placing zirconium since the other four coordinating oxygen come from the layer of oxygen atoms in Zr_2O. For the second orientation relation suggested by the NCSL model, but not experimentally observed, no periodic sites for the zirconium atom were observed for any type of oxygen coordination.

The next task in this exercise is to examine the charge neutrally. For sapphire, the aluminum atoms occupy 2/3's of the available octahedral sites. The interfacial cation layer proposed above consists of zirconium atoms occupying a different set of underlying 3-coordinated sites compared to those occupied by aluminum atoms in sapphire. For the interface proposed above, it can be shown that 3 zirconium atoms occupy the same area fraction as would normally be occupied by 4 aluminum atoms. Therefore, the interfacial cation layer, which is only composed of zirconium atoms is charge balanced by substituting 3 Zr^{4+} ions for every 4 Al^{3+} ions. Thus, charge neutrality can be achieved for the cations.

Charge neutrality for the oxygen ions will now be examined. Within the interface, two of every three oxygen atoms coordinate two zirconium atoms, while the third oxygen atom coordinates only one. In a purely ionic limit, this results in a perfect charge balance. Each oxygen atom at the interface shares –1 charge with two aluminum atoms below and therefore has another –1 for the interface. The oxygen atoms that coordinate two zirconium atoms contribute –1/2 to each atom. The oxygen atom coordinating only one zirconium atom contributes –1. This results in –2 charges for each interfacial 4+ zirconium atom, which will then receive another –2 from each of the four oxygen atoms that will coordinate it in the ensuing structure.

Although the previous paragraphs suggest that the interface is neutral, a complete charge balance must be carried out to insure that the proposed model is correct. The unit cell for sapphire is shown in Fig. 11. The cell contains 24 aluminum atoms (8 edges, 20 faces, 12 complete interior atoms) and 36 oxygen atoms (4 edges, 26 faces, and 22 complete interior atoms). The cell is terminated with oxygen atoms in the c-plane. The unit cell of cubic zirconia is shown in Fig. 12. The cell contains 12 zirconium atoms (4 edges, 12 faces, and 5 complete interior atoms) and 24 oxygen atoms (24 faces, and 12 complete interior atoms). When the two unit cells are placed together, six of the 12 terminating oxygen atoms from the ZrO_2 line up well with the terminating oxygen of the Al_2O_3. The other six oxygen atoms from the

ZrO_2 may then be removed and the six terminating oxygen atoms of the Al_2O_3 layer completed. In this manner, no atoms are incomplete and the system is charge neutral.

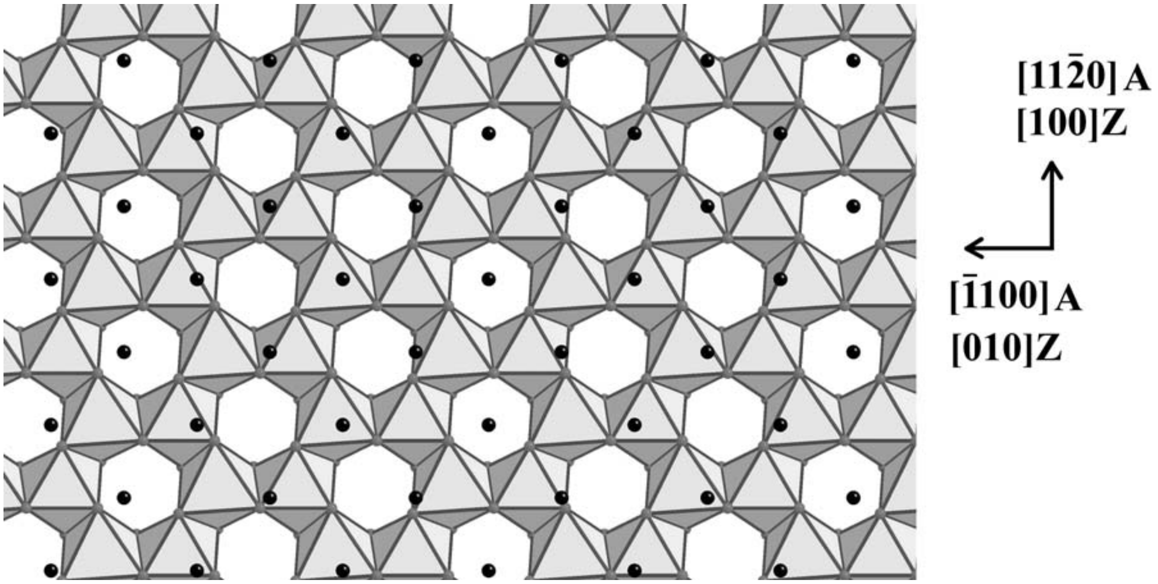

Fig. 9. The illustration shows zirconium atoms (dark black dots) from (001) ZrO_2 placed over a layer of aluminum-centered octahedrons consisting of the c-plane of sapphire. Crystallographic directions for Al_2O_3 and ZrO_2 are indicated by ‘A’ and ‘Z’ respectively.

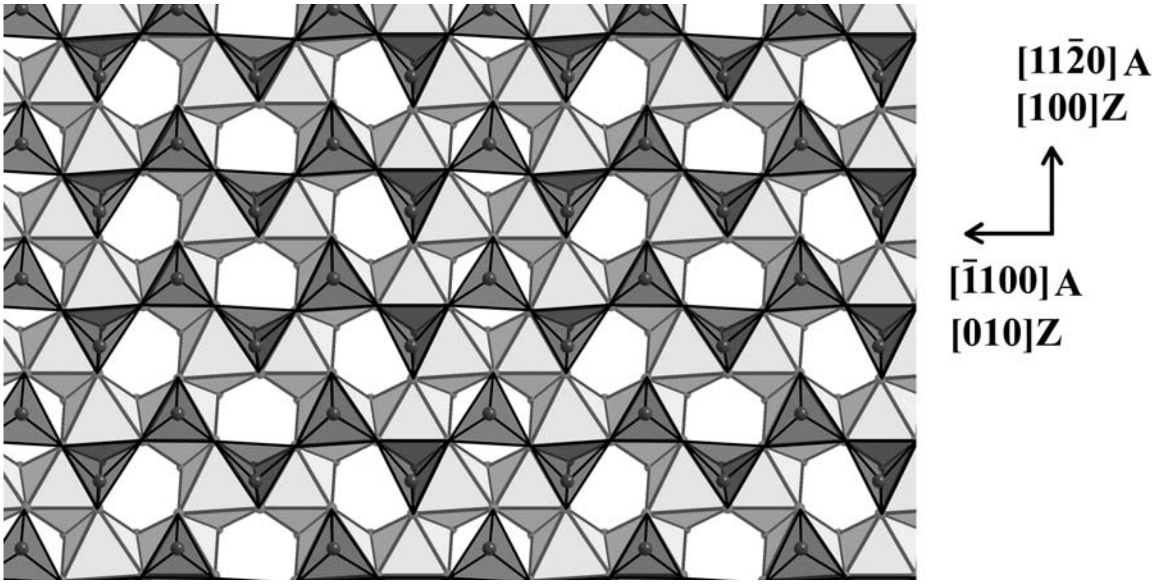

Fig. 10. A single layer of zirconium atoms scaled for a zero lattice mismatch with the underlying c-plane sapphire. The dark gray triangles show the periodic sites that become the seven-fold coordinated sites for the epitaxial interface. Crystallographic directions for Al_2O_3 and ZrO_2 are indicated by ‘A’ and ‘Z’ respectively.

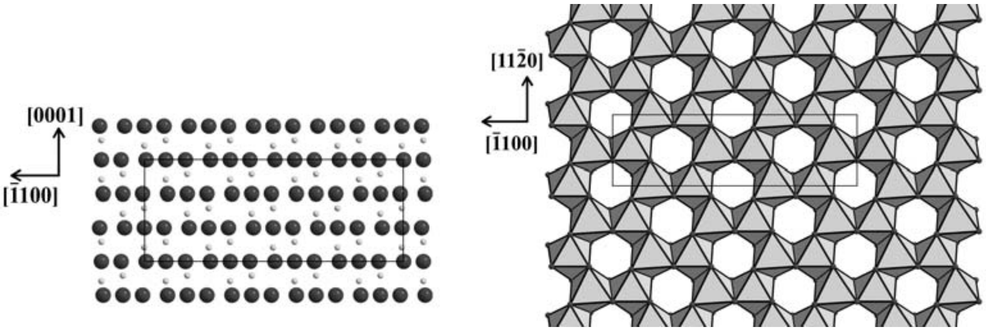

Fig. 11. (a) View of Al_2O_3, large, dark balls represent oxygen, while small, light balls represent aluminum. (b) View of c-plane sapphire, octahedra are aluminum-centered, dark lines show the unit cell selected for the charge balance analysis.

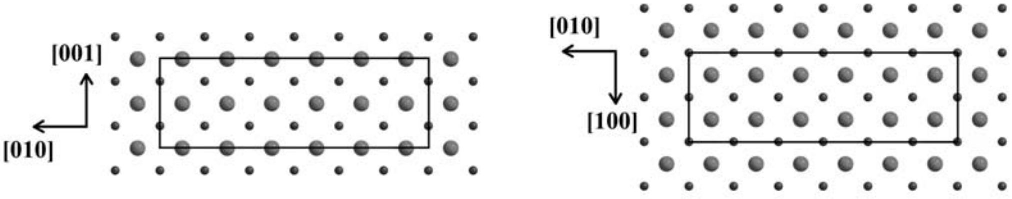

Fig. 12. (a) View of cubic ZrO_2, large, light balls represent oxygen, while small, dark balls represent zirconium. (b) View of (001) ZrO_2, the dark lines outline the unit cell used in the charge balance analysis.

Conclusion

The evidence presented above strongly suggests that the two rules of crystal chemistry, cation coordination and charge balance, can be used to explain the epitaxial relation between two different structures. These rules have been applied to four different experimentally observed epitaxial interfaces, each exhibiting a different characteristic. The $SrTiO_3$ on Ni *c*(2 X 2)S interface contains sulfur sites that stabilize the substrate interface and the subsequent epitaxial layer. Lanthanum vacancies at the anatase-$LaAlO_3$ interface allow for charge balancing and proper corner sharing of octahedra. The double oxygen layer at the rutile-(*r*-plane) sapphire interface allows for continued corner and edge sharing of octahedra as would occur in the bulk of both materials. Finally, a 7-fold coordination of cations in $Zr(Y)O_2$ provides a periodic array of available sites for its epitaxy onto c-plane sapphire. In each case, experimental results indicate that these proposed interfaces are actually observed.

Acknowledgments

This work was supported partially by the IGERT program of the National Science Foundation under Award No. DGE-9987618, and support by the U S. Department of Energy under Award No. DE-FC07-03ID14511

1. D. Andeen, L. Loeffler, N. Padture, F. F. Lange, "Crystal chemistry of epitaxial ZnO on (111) $MgAl_2O_4$ produced by hydrothermal synthesis," J. Crys. Growth, 259, 103-109, 2003.
2. S. A. Jewhurst, D. Andeen, F. F. Lange, "Crystal chemistry of the epitaxy of cristobalite (SiO_2) on basal plane sapphire," J. Crys. Growth, 280, 168-172, 2005.
3. C. Cantoni, D. K. Christen, R. Feenstra, A. Goyal, G. W. Ownby, D. M. Zehner, D. P. Norton, "Reflection high-energy electron diffraction studies of epitaxial oxide seed-layer growth on rolling-assisted biaxially textured substrate Ni (001): The role of surface structure and chemistry," Applied Physics Letters, 79 (19), 3077-3079, 2001.
4. C. Cantoni, D. K. Christen, A. Goyal, L. Heatherly, F. A. List, G. W. Ownby, D. M Zehner, H. M. Christen, and C. M. Rouleau, "Growth of Oxide Seed Layers on Ni and Other Technologically Interesting Metal Substrates: Issues Related to Formation and Control of Sulfur Superstructures

for Texture Optimization," IEEE Transactions on Applied Superconductivity, 13 (2), 2646-2650, 2003.

5. J. Y. Huang, B. H. Park, D. Jan, X. Q. Pan, Y. T. Zhu, Q. X. Jia, "High-resolution transmission electron microscopy study of defects and interfaces in epitaxial TiO_2 films on sapphire and $LaAlO_3$," Phil. Mag. A, 82 (4), 735-749, 2002.
6. M. G. Cain, F. F. Lange, "Heteroepitaxy of cubic zirconia on basal and prismatic planes of sapphire," J. Mater. Res., 9 (3), 674-687, 1994.
7. T. J. Headley, R. E. Loehman, "Crystallization of a Glass-Ceramic by Epitaxial Growth," Journal of the American Ceramic Society, 67 (9), 620-625, 1984.
8. R.W. Balluffi, A. Brokman and A.H. King, "CSL/DSC Lattice Model for General Crystal-Crystal Boundaries and Their Line Defects," Acta Metall. 30, 1453-70 (1982).
9. D. Navaco and J.P. McTague, "Orientational Epitaxy-the Orientational Ordering of Incommensurate Structures," Phys. Rev. Lett. 38, 1286 (1977).
10. J. Bohr and F. Grey, "Epitaxial Rotations and Finite Size Effect," Condensed Mat. News, 1 [3] 12-5 (1992).
11. Goyal; Amit (Knoxville, TN); Budai; John D. (Oak Ridge, TN); Kroeger; Donald M. (Knoxville, TN); Norton; David P. (Knoxville, TN); Specht; Eliot D. (Knoxville, TN); Christen; David K. (Oak Ridge, TN), "Structures having enhanced biaxial texture and method of fabricating same," United States Patent 5,739,086, April 14, 1998.
12. J. E. Demuth and T. N. Rhodin, "Chemisorption on (001), (110), and (111) nickel surfaces – A correlated study using LEED spectra, Auger spectra and work function change measurements," Surface Science 45 (1), 249-307, 1974.
13. A. Ohtomo and H. Y. Hwang, "A high-mobility electron gas at the $LaAlO_3/SrTiO_3$ heterointerface," Nature, 427, 423-426, 2004.
14. A. R. West, *Basic Solid State Chemistry*, 2nd Edition, John Wiley and Sons, 1999, p. 78.